Electronic Supplementary Material (ESI) for Journal of Materials Chemistry A.
This journal is © The Royal Society of Chemistry 2017

Electronic Supporting Information

A Self-forming Dual-phase Membrane for High-temperature Electrochemical CO_2 Capture

Peng Zhang, Jingjing Tong and Kevin Huang*

Experimental Methods

Sample preparation

The porous NiO matrix was prepared with the similar method described in our previous study.[25] Briefly, NiO powders (99.9% metal basis, Alfa Aesar) were intimately mixed in ethanol with carbon black as pore former in the volume ratios of 6:4. The dried powder mixtures were then pressed into pellets under 70 MPa, followed by sintering at 1,350 ^{o}C for 12 h in air to remove carbon pore former and achieve good mechanical strength. Thus fabricated porous NiO matrix was then impregnated with a 52 mol% Li_2CO_3-48 mol% Na_2CO_3 molten carbonate (denoted as MC) at 650 ^{o}C for 2 h to form a dense membrane. The weight increase after MC impregnation was ~20%. After MC infiltration, the surface of NiO-MC membrane was thoroughly cleaned by sandpaper.

Flux measurement

The flux densities of CO_2-O_2 permeation of the membrane were evaluated by a homemade permeation cell system as shown in Figure S1; more details on the cell assembly can be found in our early publications.[1-3] Briefly, to assemble the cell, a dense NiO-MC membrane was first sealed to a supporting alumina tube by a commercial silver paste as the sealant (Shanghai Research Institute of Synthetic Resins). A short alumina tube was then mounted to the top surface of the

NiO-MC membrane to shield the feed gas. The feed gas was a simulated flue gas, with a 100 sccm flow of the mixture containing 15%CO_2, 10%O_2 and 75%N_2; N_2 was used as a tracer gas for leak correction if any. The sweep gas was Ar flowed at 50 ml min^{-1}. The concentrations of CO_2, O_2 and N_2 in the effluent were analyzed by an on-line gas chromatographer (Agilent 490). Commercial mass flow controllers (Smart-Trak, 50 Series) specifically calibrated for each gas under use were employed to control the gas flow rates. The temperature studied was holed at 850 °C for the stability test or varied from 650 to 850 °C with a step size of 50 °C. At each temperature, ~2 h was given to allow the membrane to reach equilibrium before GC sampling. The final concentrations of CO_2, O_2 and N_2 were taken as an average of a total of consecutive 10 GC readings. The final CO_2 and O_2 flux densities (J_{CO2} and J_{O2}) were calculated by:

$$J_{CO_2} = \frac{C_{CO_2}}{(1 - C_{CO_2} - C_{O_2} - C_{N_2})} \times \frac{Q}{A} \tag{S1}$$

$$J_{O_2} = \frac{C_{O_2}}{(1 - C_{CO_2} - C_{O_2} - C_{N_2})} \times \frac{Q}{A} \tag{S2}$$

where C_{CO_2}, C_{O_2} and C_{N_2} are the measured concentrations of CO_2, O_2 and N_2, respectively; Q is the flow rate of the Ar sweep gas, *i.e.* 50 sccm; and A is the effective area of the sample, *i.e.* 0.921 cm^2.

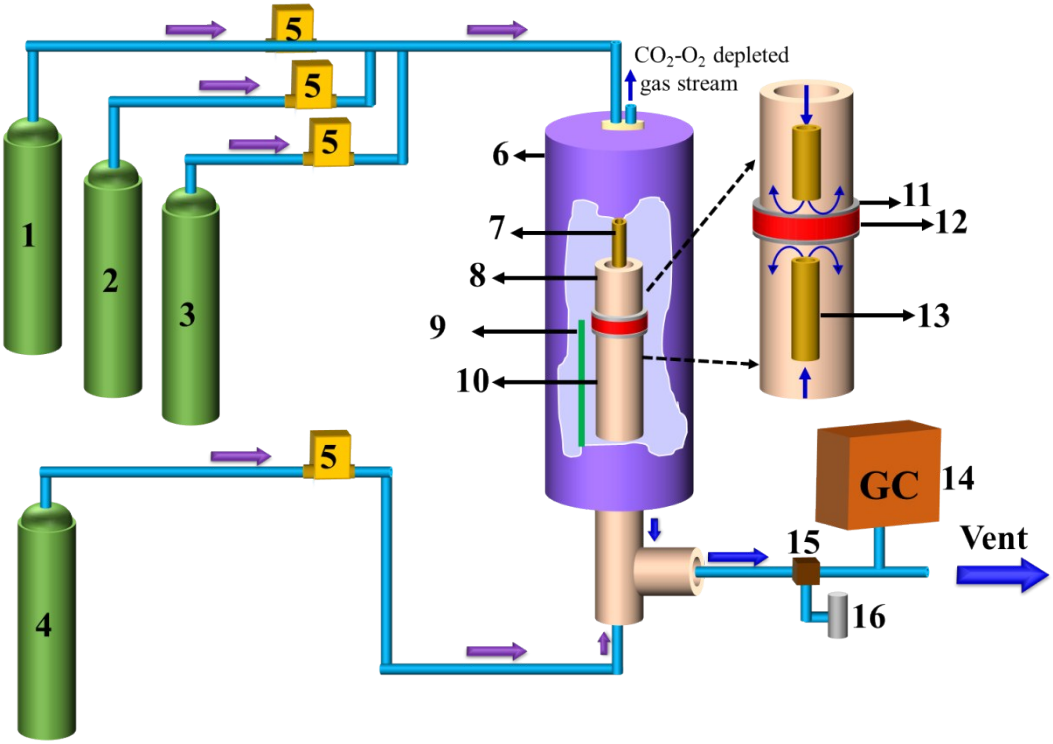

Figure S1. Schematic of the CO_2 permeation cell configurations. (1) CO_2 cylinder; (2) nitrogen cylinder; (3) oxygen cylinder; (4) argon cylinder; (5) mass flow controllers; (6) furnace; (7) inner feed tube; (8) short alumina tube; (9) thermocouple; (10) supporting alumina tube; (11) sealant; (12) NiO-MC dual-phase membrane; (13) inner sweep tube; (14) gas chromatography (GC); (15) directional-control valve and (16) soap film flowmeter.

X-ray diffraction

The room temperature phase compositions of NiO, molten carbonate (MC) and NiO-MC after firing at 850 ^{o}C were examined by an X-ray diffractometer (Rigaku, Japan) equipped with a graphite-monochromatized CuKa radiation ($\lambda = 1.5418$Å). The 2θ scans were performed at a rate of 8^{o} min^{-1} in a range of 20-90^{o}. The high-temperature XRD was performed in a temperature range of 550-800 ^{o}C in air using a high-temperature (HT) X-ray diffractometer (X1 Theta-Theta, Scintag, USA) equipped with graphite-monochromatized Cu Kα radiation ($\lambda = 1.5418$ Å) over a 2θ=20 -

90 ^{o} range in a step size of 0.02 ^{o} at a scanning rate of 1^{o} min^{-1}. During the measurement, approximately 1-h equilibrium time was given at each temperature before data collection.

SEM/STEM/EDX examination

The cross-sectional views of the NiO-MC membrane before and after testing were characterized by a scanning electron microscope (SEM) (FESEM, Zeiss Ultra) equipped with Energy dispersive X-ray spectrometry (EDX). The Focused Ion Beam (FIB， Hitachi NB-5000) technique was used to prepare sample from a post-tested NiO-MC membrane for TEM (H-9500, Hitachi) imaging and chemical analysis. The procedure to prepare FIB sample includes: 1) deposition of a carbon layer (4x12 microns) using Ga-gun on top surface of the sample; 2) deposition of a W layer (4x12 microns) using Ga-gun on top of the C layer; 3) use of 40 kV and 68.36 nA to cut around the deposited layer (see Figure S2a); 4) tilting 58 degrees and cutting at the bottom of the sample (see Figure S2b); 5) placing the sample to the original position and welding one end of the sample to a probe (see Figure S2c); 6) cutting the arm on the left side of the sample (see Figure S2d); 7) placing the sample attached to the probe on the cross sectional surface of a half TEM grid (see Figure S2e-f), followed by welding to that surface; 8) cutting off the probe (see Figure S2g); 9) thinning the cut sample (4x12x12 microns) on the TEM grid by the following condition: 40 kV and 3.55 nA to about 0.7 microns thickness; 40 kV and 0.67 nA to around 200 nm thickness; 40 kV and 0.07 nA to less than 100 nm thickness; final cleaning the cut surfaces at 5kV and 0.03 nA.

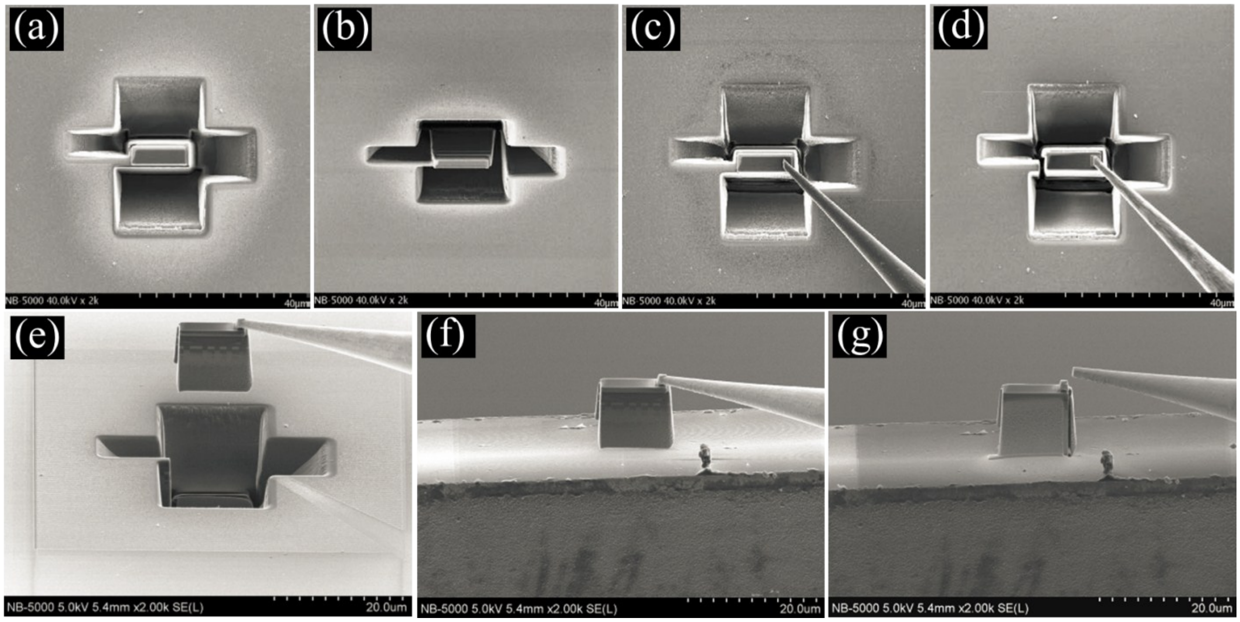

Figure S2. SEM images of the FIB process: (a) cutting around the deposited layer; (b) cutting off bottom; (c) attaching the probe; (d) cutting sample-bridge on the left arm; (e) lifting off sample; (f) attaching sample on a TEM grid; (g) cutting off probe.

Electrical conductivity measurement

The conductivity of a NiO and LNO bar sample in dimension of 25.8mm × 2.9mm × 5.0mm was measured using a standard four-probe method in air and Ar from 550 to 850 ^{o}C with the E-I module in the CorrWare software within a Solartron 1287/1260 electrochemical workstation system.

Supporting figures

A short-term stability test

Before the long-term test shown in Figure 1 of the main text, we first performed a separate short-term flux stability evaluation of the membrane. Figure S3 shows a sustainable CO_2 flux density that is ~2× the O_2 flux density during the ~40-h testing, suggesting a co-permeation process of CO_2 and O_2 by the following reaction $CO_3^{2-} = CO_2 + 1/2O_2 + e^-$. In addition, the CO_2 flux density increases from 0.78 to 1.20 mL min^{-1} cm^{-2} from the beginning to the 40-h marker, in which both CO_2 and O_2 flux densities exhibit an accelerated increase in the first 5 h, followed by a slowed increase afterwards; this behavior is thought to arise from the gradual formation of an electron conducting interphase between NiO and MC phase.

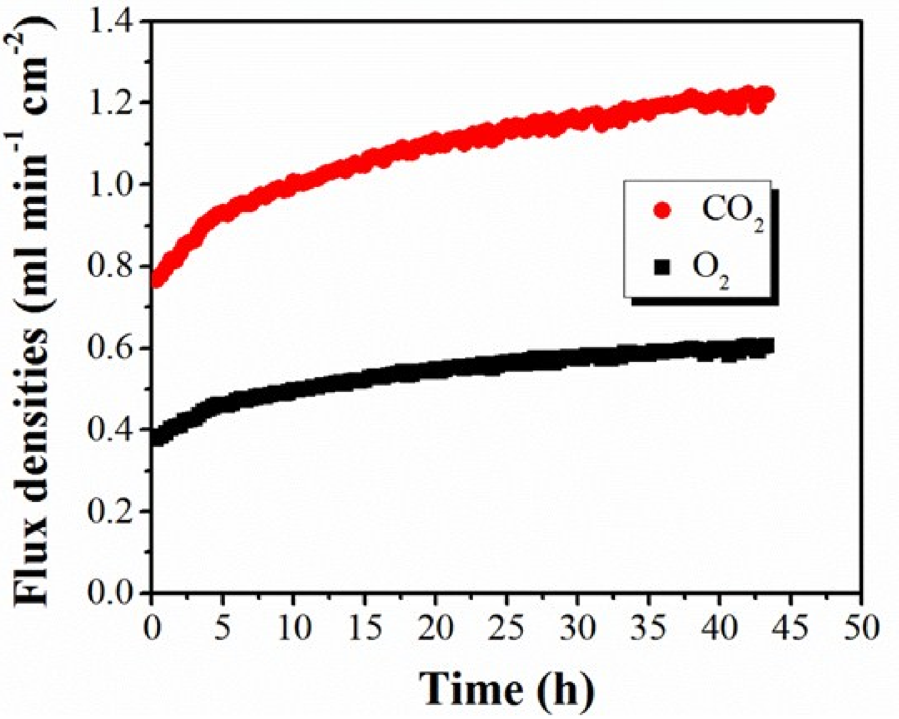

Figure S3. Short -term stability of CO_2 and O_2 flux densities in NiO-MC dual-phase membrane at 850 °C.

Microstructure and composition of the membranes before and after testing

Figure S4 shows the microstructure of the NiO-MC dual-phase membrane with a thickness of 1.2 mm after the stability test for 310 h at 850 ^{o}C shown in Figure 1. Partial MC-loss after the long-term test is visible, which is a leading cause for decrease in selectivity.

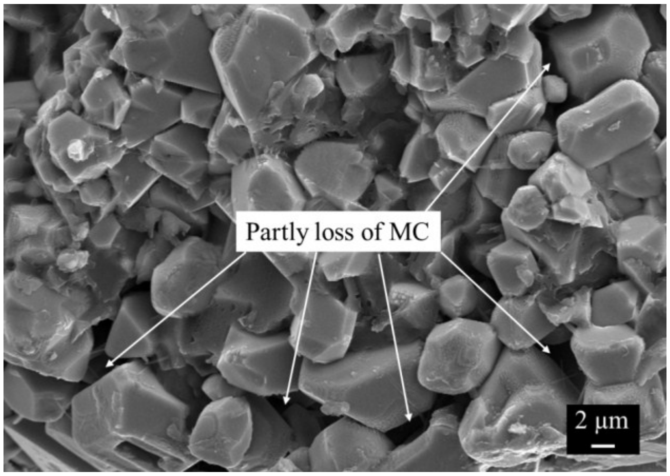

Figure S4. Microstructures of the NiO-MC membrane with a thickness of 1.2 mm after 310 h test at 850 ^{o}C.

Permeance of lithiated NiO-MC membrane vs temperature

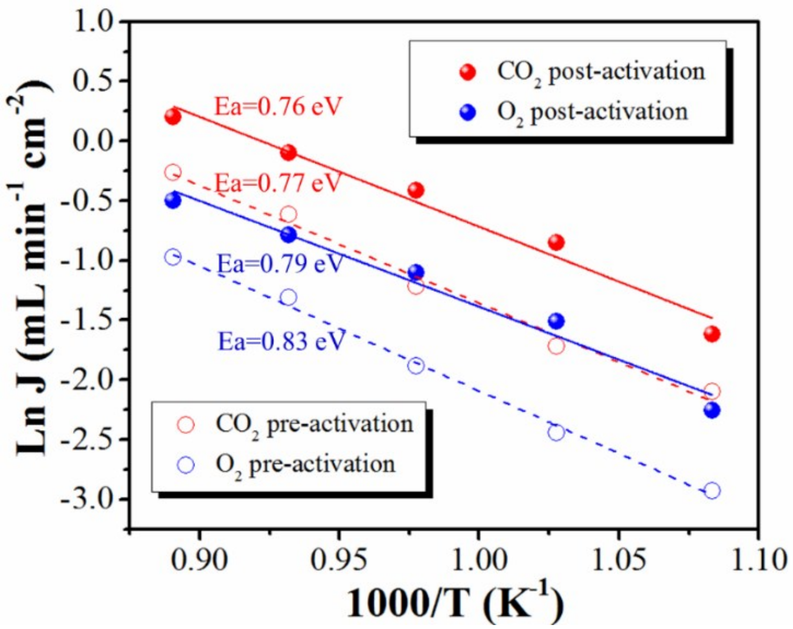

Figure S5. Arrhenius plots of the flux for lithiated NiO-MC MECC membrane before and after activation.

XRD pattern of $Li_{0.4}Ni_{1.6}O_2$

To assist in the determination of the composition of the interphase, we performed an independent XRD analysis on a sample made by firing a mixture of Li_2CO_3 and NiO in 0.22:1.60 (mol%) at 800 ^{o}C for 5 h in pure O_2. The excess Li was intentionally added to compensate the loss of Li during sintering. Figure S6 shows the XRD pattern of the reaction product, confirming the formation of a pure $Li_{0.4}Ni_{0.6}O_2$ phase. This separate study suggests that the formation of $Li_{0.4}Ni_{0.6}O_2$ phase between Li_2CO_3 and NiO can take place at lower 800 ^{o}C and shorter time, which provides complementary evidence to Figure 4 in the main context.

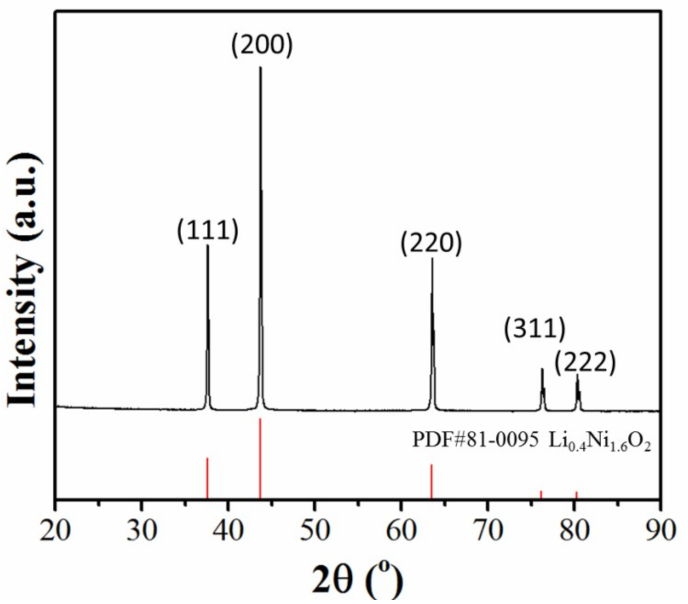

Figure S6. XRD pattern of Li_2CO_3 and NiO mixture in 0.22:1.60 (mol%) after firing at 800 °C for 5 h.

A more direct evidence of the formation of $Li_{0.4}Ni_{0.6}O_2$ phase between NiO and MC is provided by Figure S7., where a mixture of NiO and MC (1.2:1 mol%) was fired at 850°C for 10 hrs. Figure S7 of XRD pattern clearly indicates the formation of main $Li_{0.4}Ni_{0.6}O_2$ phase with residual MC phase.

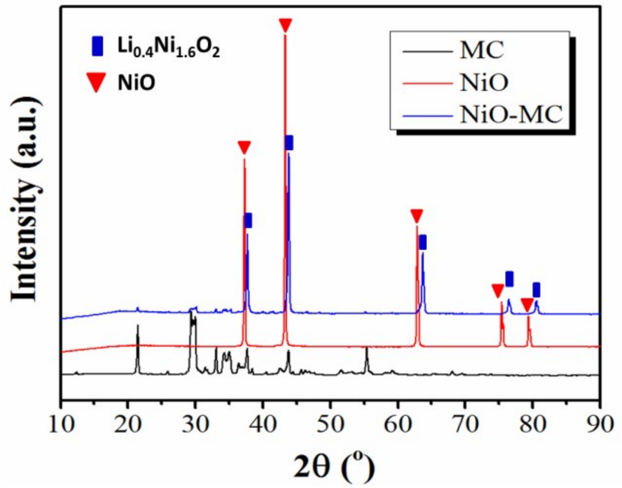

Figure S7. XRD patterns of NiO-MC mixture (molar ratio = 1:1) after firing at 850 °C for 10 h.

An *in-situ* HTXRD was also performed on a mixture of Li_2CO_3 and NiO in 0.22:1.60 (mol%) as a function of temperature; the results are shown in Figure S8. Compared to Figure 4 in the main context, the results in Figure S8 show more explicitly the formation of thermodynamically favorable LNO phase at >750^{o}C.

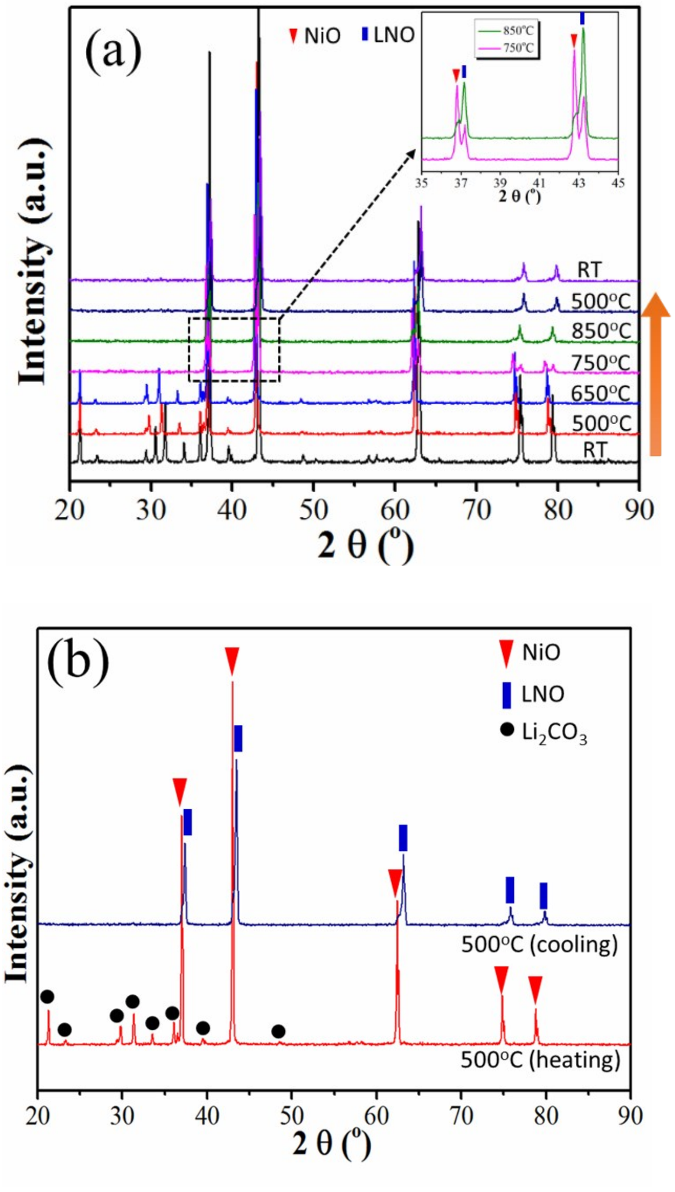

Figure S8. (a) *In situ* HT-XRD patterns of NiO and Li_2CO_3 mixture in 1.60:0.22 (mol%), collected at in air at different temperatures during heating and cooling sequence; (b) comparison of XRD patterns collected at 500 ^{o}C during heating and cooling process.

Electrical conductivity of NiO and LNO

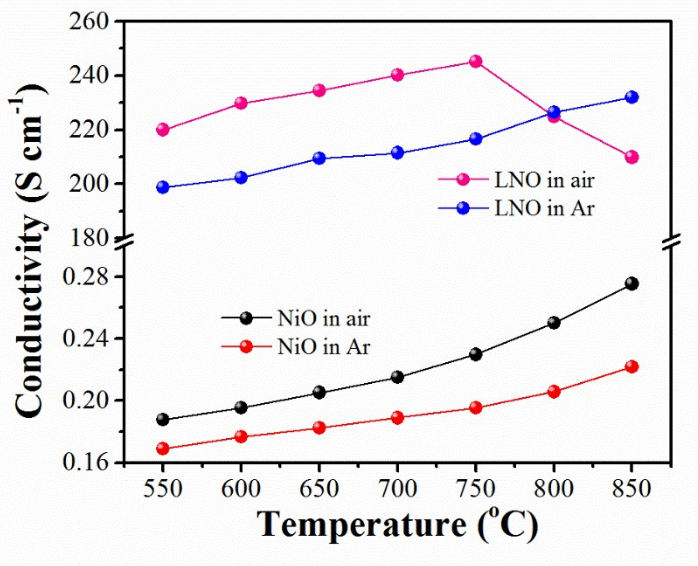

Figure S9. Electronic conductivity of NiO and LNO *vs* temperature in both air and Ar.

References:

[1] P. Zhang, J. Tong, Y. Jee, K. Huang, Chem. Commun. 2016, **52,** 9817.

[2] P. Zhang, J. Tong, K. Huang, ACS Sustainable Chem. Eng. 2016, **4,** 7056.

[3] L. Zhang, N. Xu, X. Li, S. Wang, K. Huang, W. H. Harris, W. K. S. Chiu, Energy Environ. Sci., 2012, **5,** 8310.